Andrographolide suppresses aerobic glycolysis and induces apoptotic cell death by inhibiting pyruvate dehydrogenase kinase 1 expression

EUN-SUN YANG[1*], YUNJU DO[2*], SE-YUN CHEON[1], BOSUNG KIM[2], JIN LING[2], MIN KYOUNG CHO[1], TAEKYUNG KIM[3], SUNG-JIN BAE[4] and KI-TAE HA[1,2]

[1]Korean Medical Research Center for Healthy Aging and [2]Department of Korean Medical Science, School of Korean Medicine, Pusan National University, Yangsan, Gyeongsangnam 50612; [3]Department of Biology Education, Pusan National University, Busan 46241; [4]Department of Molecular Biology and Immunology, Kosin University College of Medicine, Busan 49267, Republic of Korea

Received November 17, 2022; Accepted February 7, 2023

DOI: 10.3892/or.2023.8509

Abstract. Metabolic disorder is a major characteristic of cancer cells, and controlling genes involved in metabolic shifts can be an effective strategy for cancer treatment. Andrographolide (AG), a diterpenoid lactone, is widely recognized as a natural anticancer drug due to its ability to inhibit cancer growth. The present study aimed to investigate the mechanism underlying the mitochondrial-mediated anticancer effect of AG by inhibiting pyruvate dehydrogenase kinase 1 (PDK1) expression in lung cancer cells. Cells were treated with AG and PDK1 mRNA and protein expression was determined using reverse transcription-quantitative PCR and western blotting, respectively. As a result, AG significantly inhibited the viability of human lung cancer cells and suppressed aerobic glycolysis by decreasing lactate generation. AG further decreased the PDK1 protein and mRNA levels in a dose-dependent manner. AG-induced cell death was assessed by flow cytometry and fluorescence microscopy. AG induced apoptotic cell death that was associated with the cleavage of poly (ADP ribose) polymerase, activation of caspase-3, and mitochondrial damage, which was associated with an increase in reactive oxygen species and loss of mitochondrial membrane potential. AG-induced cell death was partially suppressed via PDK1 overexpression in lung cancer cells. Therefore, the anticancer effects of AG on human lung cancer cells may negatively regulate the expression of PDK1.

Correspondence to: Professor Ki-Tae Ha, Department of Korean Medical Science, School of Korean Medicine, Pusan National University, 49 Busandaehak Road, Yangsan, Gyeongsangnam 50612, Republic of Korea
E-mail: hagis@pusan.ac.kr

*Contributed equally

Key words: andrographolide, non-small cell lung cancer, glycolysis, pyruvate dehydrogenase kinase 1, inhibitor

Introduction

Dysregulated cellular metabolism is an emerging hallmark of cancer as it supports cellular proliferation and division via biomass generation (1,2). The most extensively researched metabolic characteristic of cancer cells is the Warburg effect, which favors glycolysis over oxidative phosphorylation (OXPHOS) to generate energy, even in the presence of sufficient oxygen (1). Genomic analysis has revealed that >70% of all human cancer cases show ubiquitous overexpression of glycolytic pathway genes (3,4). Expression levels of genes involved in glucose metabolism, including enolase 1, hexokinase 2 (*HK2*), glyceraldehyde-3-phosphate dehydrogenase (*GAPDH*), glucose transporter 1 (*GLUT1*), pyruvate kinase M2 (*PKM2*), lactate dehydrogenase A (*LDHA*), and pyruvate dehydrogenase kinase 1 (*PDK1*), are upregulated in most cancer tissues, and hence, can be used as therapeutic targets (3,5,6). The metabolic switch is directed by limiting the pyruvate utilization in the mitochondrial tricarboxylic acid (TCA) cycle, which is regulated by various cellular events, including altered growth factor signaling, hypoxic or normoxic activation of hypoxia-inducible factor 1α (HIF1α), oncogene activation and loss-of-function of suppressor genes (5,7).

Andrographolide (AG), a diterpenoid lactone, was first identified in *Andrographis paniculata* (Burm.f.) Nees, an annual herbaceous plant belong to the *Acanthaceae* family, commonly referred to as 'green chiretta' (8). AG is widely accepted as a natural anticancer agent owing to its ability to inhibit cancer growth and induce apoptotic cell death (9). Several cellular pathways, including Wnt/β-catenin, phosphatidylinositol-3-kinase (PI3K)-mammalian target of rapamycin, vascular endothelial growth factor-mediated signaling, and tumor necrosis factor-related apoptosis-inducing ligand-mediated apoptosis pathways, have been identified as key pathways regulated by AG (9,10). AG directly binds to Ras and nuclear factor-κB and lowers their expression levels or activities (11,12).

AG targets HIF1α by downregulating its expression or stability, thereby inhibiting its DNA-binding activity (13-16). Recently, two separate groups have shown that AG inhibits the glycolytic metabolic profile of cancer cells by controlling the expression of enzymes involved in glycolysis, including GLUT1, HK2, phosphofructokinase 1 (PFK1), PKM2 and LDHA (17,18). The molecular mechanism by which AG suppresses aerobic glycolysis has not yet been fully characterized.

In the present study, it was found that AG suppressed aerobic glycolysis and induced mitochondria-mediated apoptosis in human lung cancer cells. In addition, AG decreased the expression levels of several PDKs, including PDK1. Apoptotic cell death was reduced in PDK1-overexpressing cells. Based on these findings, it was hypothesized that the pro-apoptotic activity of AG may be mediated by the negative regulation of PDK1 expression.

Materials and methods

Materials. AG was purchased from the Tokyo Chemical Industry. A 100 mM stock solution of AG was dissolved in dimethyl sulfoxide (DMSO) and stored at -20˚C. AG was diluted to the appropriate concentration with a final DMSO concentration of less than 0.1%. All other chemicals, including DMSO, sodium dodecyl sulfate (SDS), Tween 20, and 3-(4,5-dimethyl-thiazole-2-yl)2,5-diphenyl tetrazolium bromide (MTT), were purchased from MilliporeSigma. All antibodies used in the present study for western blotting are listed in Table I. Roswell Park Memorial Institute (RPMI)-1640 medium, 1X phosphate-buffered saline (PBS; pH 7.4), and 0.25% trypsin-ethylenediaminetetraacetic acid (EDTA) were obtained from Welgene, Inc. Fetal bovine serum (FBS) and penicillin/streptomycin were obtained from Gibco; Thermo Fisher Scientific, Inc.

Cell lines and cultures. Human non-small cell lung cancer (NSCLC) cell lines, namely A549 (adenocarcinoma), NCI-H292 (H292; mucoepidermoid carcinoma) and NCI-H522 (H522; adenocarcinoma), were obtained from the Korean Cell Line Bank (Seoul, Korea). Cells were cultured in RPMI-1640 medium supplemented with 10% FBS and 1% penicillin/streptomycin in a 5% CO_2 incubator at 37˚C under 98% humidified conditions.

Cell viability assay. Cell viability was determined via the MTT (dissolved in DMSO) assay. Cells ($1x10^4$ cells/well) were initially seeded into a 96-well culture plate in triplicate, followed by treatment with various concentrations of AG (10, 20, 50 and 100 μM) the next day in a fresh medium. After 24 h of incubation, MTT solution (5 mg/ml) was diluted in culture medium and added to each well of the plate to a final concentration of 0.5 mg/ml, and the culture plate was further incubated at 37˚C for 4 h. Absorbance was measured at 540 nm using the Spectramax M2 microplate reader (Molecular Devices, LLC).

Lactate production assay. Lactate production in H292 cells was measured using the lactate fluorometric assay kit (BioVision, Inc.). Briefly, $1x10^4$ cells/well were seeded into a 96-well plate and incubated overnight at 37˚C. Prior to pretreatment with various concentrations of AG (20, 50 and 75 μM), the medium was replaced with phenol red and serum-free RPMI medium and incubated at 37˚C for 1 h. Finally, 1 μl of the medium from each well was received to measure the absorbance at 570 nm using the Spectramax M2 microplate reader (Molecular Devices, LLC).

Western blot analysis. After incubation, the cells were harvested and lysed in ice-cold 1% NP-40 lysis buffer containing 150 mM NaCl, 10 mM HEPES (pH 7.45), 5 mM sodium pyrophosphate, 5 mM sodium fluoride, 2 mM sodium orthovanadate, and a protease inhibitor cocktail (Roche Applied Science). Whole cell extracts were obtained from the supernatants after centrifugation of the cell lysate at 13,000 x g for 15 min at 4˚C. Protein concentration was quantitated using the Bradford assay. Proteins (50 μg) were separated via SDS-polyacrylamide gel electrophoresis (PAGE; 8-13%) and transferred onto 0.45 μM nitrocellulose membranes (Amersham; Cytiva). The membranes were blocked for 60 min at room temperature using 5% (w/v) BD Difco skim milk powder (Thermo Fisher Scientific, Inc.) and immunoblotted with primary antibodies at 4˚C overnight at optimal dilution (Table I). After washing three with Tris-buffered saline with 0.1% Tween 20 buffer, the membranes were incubated with horseradish peroxidase-conjugated secondary antibodies at a dilution of 1:2,000 for 1 h at room temperature. Immunoreactivity was detected using ECL Plus (Amersham; Cytiva) and digitalized using Image Quant LAS 4000 (GE Healthcare).

In vitro PDK activity assay. Kinase activity of PDK was slightly modified as previously described (19,20). Briefly, 50 ng of recombinant PDK1 (Abcam) was incubated with 100 ng of recombinant pyruvate dehydrogenase E1 subunit alpha 1 (PDHA1; Abcam) for 30 min at 37˚C in PDK1 buffer containing 20 mM Tris buffer (pH 7.5), 0.1 mM EDTA, 1 mM $MgCl_2$, 2 mM dithiothreitol (DTT) and 250 μM ATP. The samples were subjected to SDS-PAGE and immunoblotted using antibodies against PDK1, p-PDHA1, and PDHA1 (Table I).

Reverse transcription-quantitative polymerase chain reaction (RT-qPCR). Total RNA was isolated from H292 cells using the TRIZOL® reagent (Invitrogen; Thermo Fisher Scientific, Inc.) and quantified at 260 nm wavelength using the Nanodrop 2000 spectrophotometer (Thermo Fisher Scientific, Inc.), according to the manufacturers' instructions (21). An equal amount of RNA (1 μg) from each sample was used to synthesize cDNA, which was reverse-transcribed using RevertAid reverse transcriptase (cat. no. EP0441; Thermo Fisher Scientific, Inc.). RT was performed according to the manufacturer's instructions. qPCR was performed using the StepOnePlus real-time PCR system (Applied Biosystems; Thermo Fisher Scientific, Inc.) with the RealHelix qPCR kit (cat. no. QP2-S500; NanoHelix Co., Ltd.). PCR was performed with initial denaturation at 95˚C for 15 min, followed by 40 cycles of the reaction at 95˚C for 20 sec, 60˚C for 30 sec, and 72˚C for 30 sec. Relative mRNA levels were normalized to actin levels. All the primers used in the present study are listed in Table II.

Flow cytometric analysis. Apoptotic cells were examined using the Annexin V-fluorescein isothiocyanate (FITC) Apoptosis Detection Kit (Thermo Fisher Scientific, Inc.).

Table I. List of antibodies used in the present study.

Antibody	Company	Cat. no.	Dilution factor
Phosphorylated PDHA1	Abcam	ab177461	1:1,000 in 2% skim milk
PDHA1	Santa Cruz Biotechnology, Inc.	sc-377092	1:2,000 in 5% skim milk
PDK1	Enzo Life Sciences, Inc.	ADI-KAP-PK112	1:2,000 in 5% skim milk
PDK2	Signalway antibody LLC	41330	1:1,000 in 5% skim milk
PDK3	Novus Biologicals, LLC	NBP1-32581	1:1,000 in 5% skim milk
PDK4	Signalway antibody LLC	38562	1:1,000 in 5% skim milk
GAPDH	Santa Cruz Biotechnology, Inc.	sc-32233	1:2,000 in 5% skim milk
PARP	Cell Signaling Technology, Inc.	9542	1:1,000 in 5% skim milk
Cleaved Caspase-3	Cell Signaling Technology, Inc.	9661	1:1,000 in 2% skim milk
Caspase-9	Cell Signaling Technology, Inc.	9508	1:1,000 in 2% skim milk
HSP90	Santa Cruz Biotechnology, Inc.	sc-13119	1:2,000 in 5% skim milk
Anti-mouse IgG	Invitrogen; Thermo Fisher Scientific, Inc.	RJ240410	1:2,000 in 5% skim milk
Anti-rabbit IgG	Invitrogen; Thermo Fisher Scientific, Inc.	SA245916	1:2,000 in 5% skim milk

PDK, pyruvate dehydrogenase kinase.

Table II. List of primers used in the present study.

Gene name	Primer sequence (5'→3')
PDK1 cloning	F: AAGAATTCCATGAGGCTGGCGCGGCTGC
	R: ACCTCGAGCTAGGCACTGCGGAACGTCG
PDK1	F: CTATGAAAATGCTAGGCGTCT
	R: AACCACTTGTATTGGCTGTCC
PDK2	F: AGGACACCTACGGCGATGA
	R: TGCCGATGTGTTTGGGATGG
PDK3	F: GCCAAAGCGCCAGACAAAC
	R: CAACTGTCGCTCTCATTGAGT
β-actin	F: CAAGAGATGGCCACGGCTGCT
	R: CACAGGACTCCATGCCCAGGA

PDK, pyruvate dehydrogenase kinase; F, forward; R, reverse.

Cells ($3x10^5$ cells/well) were seeded into a six-well plate and incubated overnight at 37˚C. The next day, cells were treated with various concentrations of AG (20, 50, and 75 μM) for 24 h and resuspended in 500 μl of binding buffer (1X) to obtain a cell density of $2x10^5$ cells/ml. The cells were then incubated with 5 μl of Annexin V-FITC and 10 μl propidium iodide (PI; 20 μg/ml) in cell suspension for 15 min at room temperature. Fluorescence intensities of the samples were determined using the FACS Canto II flow cytometer (BD Biosciences). In the histogram of FACS analysis, apoptotic cells were represented the combination of Q2 (PI^+/Annexin V^+, late apoptotic cell) and Q3 (PI^-/Annexin V^+, early apoptotic cell), and dead cells were represented the combination of Q1 (PI^+/Annexin V^-, necrotic cell) and Q2 (PI^+/Annexin V^+, late apoptotic cell).

Determination of mitochondrial reactive oxygen species (ROS) levels. The production of intracellular mitochondrial ROS was determined using MitoSOX Red (Invitrogen; Thermo Fisher Scientific, Inc.). Briefly, 1 μM MitoSOX Red was added to the cultured cells in conditioned medium and incubated at 37˚C for 10 min. Fluorescence intensity was determined using a fluorescence microscope (AX10 Imager M1; Zeiss AG) and calculated using the ImageJ software (version 1.53; National Institutes of Health).

Measurement of mitochondrial membrane potential (MMP). Cells ($3x10^5$ cells/well) were seeded into a six-well plate and incubated overnight at 37˚C. The next day, the cells were treated with various concentrations of AG (20, 50 and 75 μM) for 12 h and incubated with 250 nM tetramethylrhodamine methyl ester (TMRM; Thermo Fisher Scientific, Inc.) for 30 min. The cells were washed thrice with PBS and observed under a fluorescence microscope (AX10 Imager M1). Membrane depolarization was determined by analyzing the captured images using the ImageJ software (version 1.53; National Institutes of Health).

Plasmid preparation and transfection for PDK1 overexpression. PCR product of PDK1 was ligated into the pMX-IRES-puromycin vector containing *Eco*RI and *Xho*I restriction enzyme sites. The primers used to clone the PDK1 construct are listed in Table II. Plat-A cells, a retroviral packaging cell line, were transfected with 1 μg of pMX-IRES empty vector (EV) and pMX-IRES-PDK1 vector (PDK1-OE) using Lipofectamine 2000 (Invitrogen; Thermo Fisher Scientific, Inc.). The supernatant was collected after 24 h, and the culture medium of H292 cells was replaced with filtered retroviral supernatant containing 5 μg/ml polybren (Santa Cruz Biotechnology, Inc.). The cells were selected using 2 μg/ml puromycin after viral infection for 24 h and cultured for an additional 2 weeks.

Bioinformatics analysis. The known target gene list of AG was downloaded from PubChem (https://pubchem.ncbi.nlm.nih.gov/#query=andrographolide) and analyzed using Cytoscape's JEPPETTO plugin (https://apps.cytoscape.org/apps/jepetto). Kyoto Encyclopedia of Genes and Genomes analysis (https://www.genome.jp/kegg/) identified several cancerous, metabolic and p53 signaling pathways as AG-related pathways. Interaction between genes and chemicals by AG were analyzed using BioCarta Pathways Dataset (https://maayanlab.cloud/Harmonizome/search?t=all&q=andrographolide). The GSE74769 microarray dataset (obtained from the Gene Expression Omnibus database; https://www.ncbi.nlm.nih.gov/geo/) was examined to identify a potential link between glycolysis and AG. The correlation between PDK mRNA expression and AG cytotoxicity in the cells was performed using Spearman's correlation analysis.

Statistical analysis. All data are from at least three independent experiments and expressed as the mean ± standard deviation. Statistical differences were calculated via one-way analysis of variance with Dunnett's post hoc test or unpaired Student's t-test. GraphPad Prism software (version 5.0; GraphPad Software, Inc.) was used for all statistical analyses, and $P<0.05$ was considered to indicate a statistically significant difference.

Results

Cytotoxic effect of AG is related to PDK1 expression. To validate the molecular pathways related to AG, the known target gene list was downloaded from PubChem (https://pubchem.ncbi.nlm.nih.gov/#query=andrographolide) and analyzed using Cytoscape's JEPPETTO plugin (https://apps.cytoscape.org/apps/jepetto). Kyoto Encyclopedia of Genes and Genomes analysis (https://www.genome.jp/kegg/) identified several cancerous, metabolic and p53 signaling pathways as AG-related pathways. BioCarta analysis (https://maayanlab.cloud/Harmonizome/search?t=all&q=andrographolide)revealed that the p53, DNA damage, cell cycle, apoptosis, and HIF pathways are involved in AG treatment (Tables SI-SIII). Pathway analysis revealed no direct evidence of a connection between glucose metabolism and AG. Next, the GSE74769 microarray dataset (obtained from the Gene Expression Omnibus database; https://www.ncbi.nlm.nih.gov/geo/) was examined to identify a potential link between glycolysis and AG. The results clearly revealed that AG treatment downregulated the expression levels of numerous genes involved in pyruvate metabolism. Among them, focus was addressed on *PDK1*, a key regulator of pyruvate metabolism (22), as its levels were reduced by >50%, similar to the previously reported genes, including *HK2*, *PFK1* and *LDHA* (Fig. S1) (17,18).

Next, the cytotoxic effects of AG were confirmed on several NSCLC cell lines, namely the A549, H292 and H522 cell lines. It was found that AG caused more severe cytotoxicity in H292 and H522 cells than that in A549 cells (Fig. 1). The GI_{50} (concentration for 50% of maximal inhibition of cell proliferation) of each cell line was 102.28 μM for A459, 46.17 μM for H292, and 43.59 μM for H522. Examination of the Spearman's correlation between PDK mRNA expression and AG cytotoxicity in these cell lines revealed that PDK1 was most closely related to AG cytotoxicity (Fig. S2), whereas PDK4 expression was lacking in these cell lines. H292 and H522 cells demonstrated higher PDK1 expression than A549 cells at the protein level (Fig. S3A) as well as the mRNA level. Furthermore, AG exhibited strong cytotoxicity in HCT116 and DLD-1 cells with high PDK1 expression (Fig. S3). These findings suggested that PDK1 may be involved in AG-induced cytotoxicity in cancer cells.

AG reduces the protein expression levels of PDK1, 2 and 3. Pyruvate, the end product of glycolysis, can be converted to lactate in the cytosol or to acetyl CoA to enter the TCA cycle in mitochondria. Therefore, the effects of AG on metabolic pathways following pyruvate synthesis were verified. Similar to a recent study (17), AG decreased lactate generation in a dose-dependent manner in H292 cells (Fig. 2A). The protein expression of LDHA, an enzyme that catalyzes the conversion of pyruvate to lactate, was unchanged (Fig. 2B). AG significantly decreased the phosphorylation of PDHA1, an enzyme that converts pyruvate to acetyl-CoA (Fig. 2B). Because the phosphorylation of PDHA1 is regulated by PDKs, the protein expression levels of PDKs were examined. As expected, AG induced a decrease in the protein expression levels of PDK1, 2 and 3 in a dose-dependent manner in H292 cells (Fig. 2C). In particular, the expression of PDK1 was markedly reduced. To confirm that AG directly controlled the activity of PDK1, an *in vitro* PDK activity assay was performed using recombinant proteins for protein binding. However, AG did not directly bind to PDK1 (Fig. 2D). Some binding inhibition was observed at a high concentration of 10 μM or more, which was comparable to the intracellular working concentration (20 μM). The positive control, dichloroacetate, demonstrated a binding inhibitory effect, even at a concentration of 1 mM, which was substantially lower than the intracellular working concentration (10 mM). AG not only decreased the protein expression levels of PDK1, 2 and 3 but also decreased their mRNA levels in a dose-dependent manner in H292 cells (Fig. 2E-G). These findings suggested that AG was involved in the regulation of the mitochondrial metabolic pathways by inhibiting the conversion of pyruvate to acetyl-CoA via a decrease in PDK1 expression.

AG promotes apoptotic cell death via mitochondrial ROS generation and loss of MMP. Metabolic reprogramming of cancer cells from aerobic glycolysis to OXPHOS promotes mitochondrial ROS-dependent cell death (23,24). Thus, it was investigated whether AG induced apoptotic cell death and mitochondrial dysfunction in H292 and A549 cells, wherein different PDKs were expressed and different cytotoxicities were observed (Fig. 1). When the number of AG-induced apoptotic cells after Annexin V-FITC and PI staining was measured via FACS analysis, it was found that the number of A549 cells was weakly increased, whereas the number of H292 cells was significantly increased during apoptosis (Fig. 3A and B). Similar results were obtained in the histogram analyzed using the ImageJ software (Fig. 3C). Levels of cleaved caspase-3, cleaved caspase-9 and PARP, which are proteins involved in the apoptotic signaling pathway, were also increased in AG-treated H292 cells, but not in A549 cells, in a dose-dependent manner (Fig. 3D).

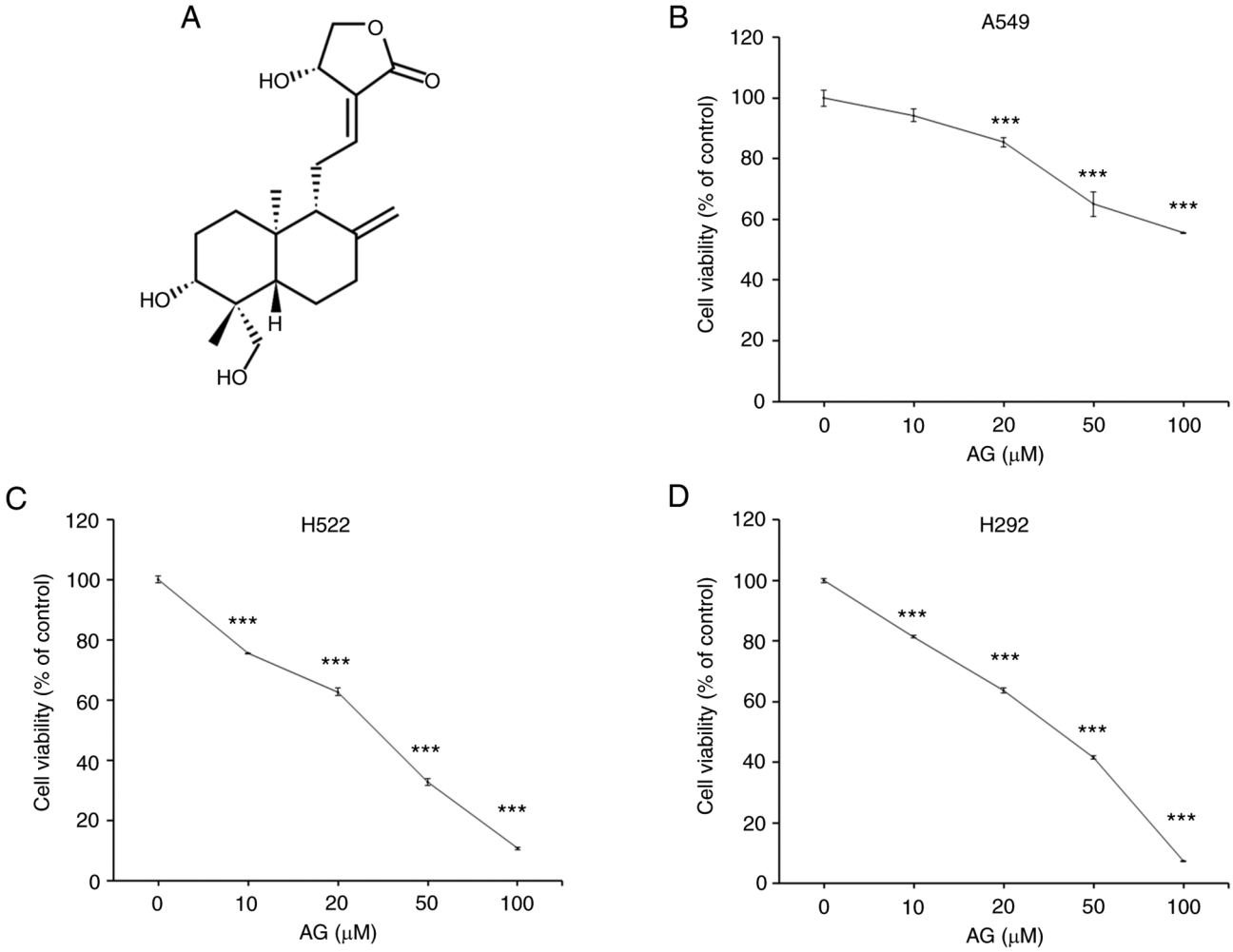

Figure 1. AG increases the cellular toxicity in non-small cell lung cancer cell lines. (A) Molecular structure of AG. (B-D) Cytotoxic effect of AG was highly potent in H292 and H522 cells but relatively weak in A549 cells. ***P<0.001. AG, andrographolide.

AG remarkably increased the generation of mitochondrial ROS in H292 cells, as determined via MitoSOX staining (Fig. 4A). As revealed in the histogram of the relative amount of AG-induced mitochondrial ROS production (Fig. 4C), a significant increase in ROS levels was observed in H292 cells. TMRM staining assay revealed that AG reduced the MMP in H292 cells in a dose-dependent manner (Fig. 4B). Histogram analysis revealed that AG decreased the MMP in H292 cells but not in A549 cells (Fig. 4D). These results suggested that AG-induced metabolic shift can lead to apoptotic cell death in H292 cells by increasing mitochondrial ROS levels and depleting the MMP.

Cytotoxic effect of AG is influenced by PDK1 expression. To determine whether the inhibition of PDK1 expression by AG is critical for cancer cell death, a PDK1-overexpressing (PDK1-OE) cell line was constructed by transfecting a virus with its expression vector. As revealed in Fig. 5A, the PDK1 protein was overexpressed in H292 cells, as determined by western blotting. PDK1 mRNA was overexpressed in H292 cells, as determined by RT-qPCR (Fig. 5B). In addition, AG-induced cytotoxicity in the MTT assay was significantly suppressed in PDK1-overexpressed H292 cells than that in the EV cells (Fig. 5C). At the highest concentration of AG (75 μM), only 7.68% of empty vector cells survived, and 31.7% of PDK1-overexpressed cells survived. The morphological changes in PDK1-overexpressing H292 and EV cells after treatment with AG are demonstrated in Fig. 5D. In PDK1-overexpressing H292 cells, AG-induced cytotoxicity was relatively weak compared with that in the control (EV) cells. Histogram also revealed that the number of AG-induced dead cells was slightly reduced in PDK-overexpressing H292 cells compared with that in the control cells (Fig. 5E). Expression of apoptotic marker proteins, including cleaved-PARP and cleaved-caspase 3, was suppressed in PDK1-overexpressing H292 cells (Fig. 5F). These results indicated that PDK1 expression was partially involved in the cytotoxic effects of AG. By suppressing PDK1 expression with AG, the metabolic shift from glycolysis to OXPHOS caused a significant increase in mitochondrial ROS generation, which is another key factor for AG-induced cancer cell death (Fig. 5G).

Discussion

PDH complex connects glycolysis to mitochondrial OXPHOS by converting pyruvate to acetyl-CoA, the main substrate of TCA cycle (25). PDH activity is inhibited by PDKs through phosphorylating serine residues in its E1 subunit

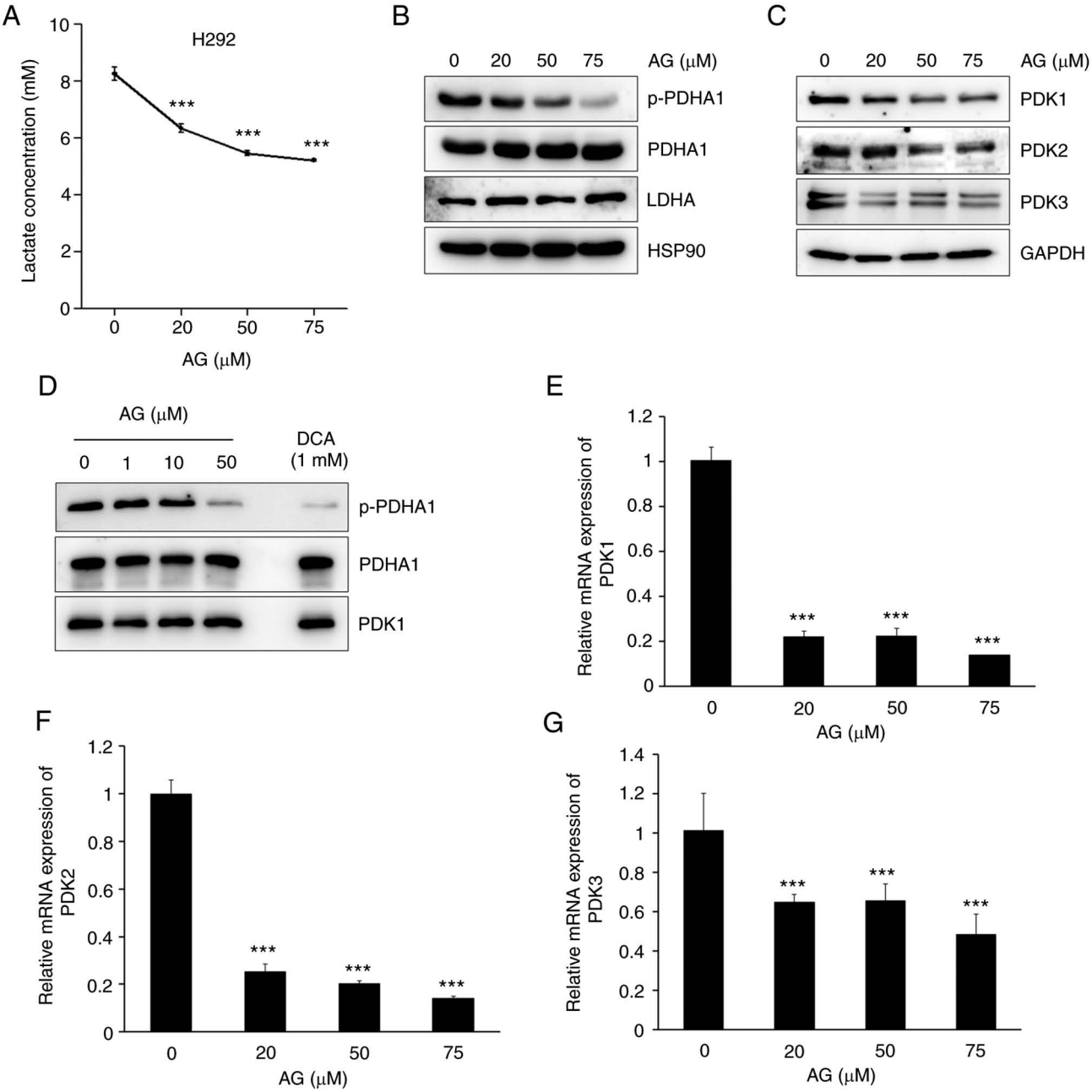

Figure 2. AG inhibits the PDK protein and mRNA expression. (A) H292 cells were treated with AG at the indicated doses for 1 h. (A) AG reduced lactate generation in a dose-dependent manner. (B) AG significantly inhibited the expression of p-PDHA1, which is phosphorylated by PDKs. Total amount of PDHA1 was not changed by AG treatment. Expression of LDHA also was not affected by AG treatment. HSP90 represents the normalized control of each well. (C) After H292 cells were treated with various concentrations of AG (20, 50 and 75 μM) for 6 h, the protein expression levels of mitochondrial PDK1, PDK2, and PDK3 were determined via western blotting. GAPDH represents the normalized control of each well. Protein expression levels of PDKs decreased in a dose-dependent manner after AG treatment. Notably, PDK1 expression levels significantly decreased after AG treatment. (D) *In vitro* PDK activity assay was performed to determine whether PDK1 activity was regulated by AG. AG did not directly regulate the activity of PDK1. (E-G) H292 cells were treated with various concentrations of AG (20, 50 and 75 μM) for 6 h, and the mRNA levels of PDK1, PDK2 and PDK3 were determined via reverse transcription-quantitative polymerase chain reaction. AG significantly decreased the mRNA levels of PDKs in H292 cells. Data are represented as the mean ± standard deviation compared with the control from three independent experiments. ***P<0.001 vs. control. AG, andrographolide; PDK, pyruvate dehydrogenase kinase; PDHA1, pyruvate dehydrogenase E1 subunit alpha 1; LDHA, lactate dehydrogenase A; HSP90, heat shock protein 90; GAPDH, glyceraldehyde 3-phosphate dehydrogenase; p-, phosphorylated.

(PDHA1) (22,26). Thus, PDKs are suggested to be master regulators of aerobic glycolysis because they limit pyruvate carboxylation to acetyl-CoA, thereby facilitating pyruvate reduction to lactate (7,25). PDK1 is the most critical enzyme for the development and metastasis of various types of malignant cancer (25,27-30), particularly NSCLC (31). Several PDK1 inhibitors, such as dichloroacetate (DCA), AZD 7545, and 2,2-Dichloro-1-(4-isopropoxy-3-nitrophenyl)ethan-1-one (Cpd64), have been studied to develop novel cancer therapies (32-34). The use of several natural compounds as PDK1 inhibitors and anticancer agents in various cancer types have been also reported, including NSCLC (35-37). Initially, AG was expected to inhibit PDK1 activity and expression. However, the *in vitro* PDK activity assay revealed that AG had a very

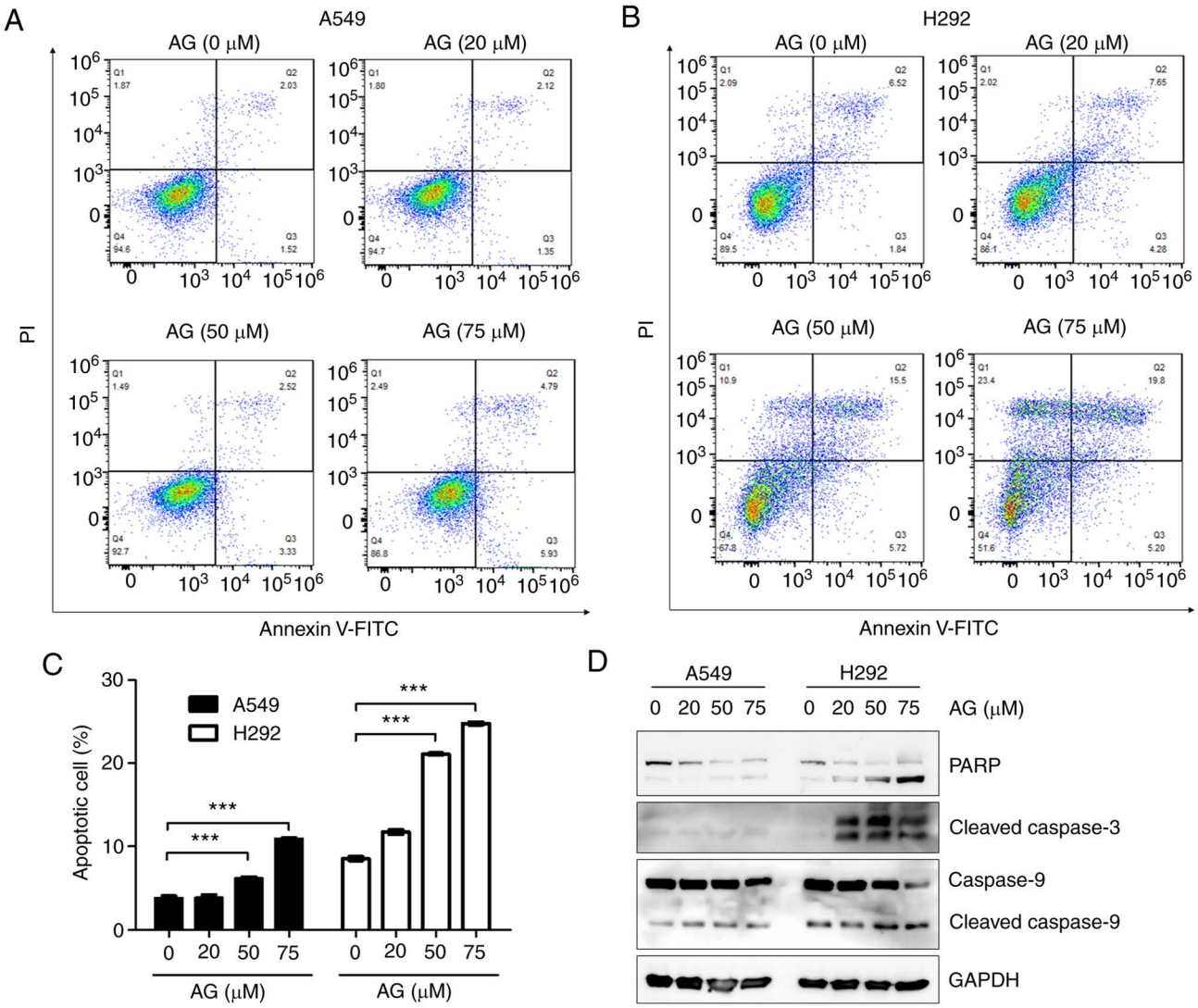

Figure 3. AG induces more apoptotic cell death in H292 cells than A549 cells. (A and B) A549 and H292 cells were treated with various concentrations of AG (20, 50 and 75 μM) for 6 h, labeled with Annexin V-fluorescein isothiocyanate and propidium iodide, and analyzed via flow cytometry. (C) Histogram showing the percentage of apoptotic cells. Apoptotic cells were quantified by combining Q2 (late-stage of apoptotic cells, PI^+/Annexin V^+) and Q3 (early-stage of apoptotic cells, PI^-/Annexin V^+) regions after FACS analysis. AG significantly increased the apoptotic cell death in H292 cells, but not in A549 cells, in a dose-dependent manner. (D) To determine the protein levels of PARP, cleaved caspase-3, and cleaved caspase-9 via western blot analysis, A549 and H292 cells were treated with AG at the indicated dose for 24 h. Levels of all apoptotic marker proteins were significantly increased by AG treatment in H292 cells and only slightly increased in A549 cells. Data are represented as the mean ± SD compared with the control from three independent experiments. ***P<0.001 vs. control. AG, andrographolide; PARP, cleaved poly (ADP ribose) polymerase.

low inhibitory effect on PDK1 activity. Recent metabolomic research has revealed an increase in the levels of TCA cycle metabolites, including citrate, cis-aconitic acid, and isocitrate, as well as glycolytic metabolites in AG-treated red blood cells (RBCs) (38). Since mature RBCs do not synthesize RNA or proteins, the metabolites can reflect the activity of glycolytic and TCA cycle enzymes. The present findings are consistent with the aforementioned study, as AG did not have any effect on the enzyme activity.

PDK expression levels are tightly regulated by several upstream regulators. The most well-known upstream regulator of PDK expression is HIF1α, which also increases the expression levels of other glycolytic enzymes, including GLUT1, HK2, PKM and LDHA (26,39). HIF1α activates PDK1 and PDK3. It is part of a series of reactions to achieve a low-oxygen state by actively decreasing the mitochondrial oxygen consumption via the induction of PDK expression and inhibition of PDH activity (40). Other upstream regulators, including transcription factors E2F1, Myc and Wnt, have been linked to PDK expression, particularly PDK1 and PDK3 (41-43). The expression levels of PDK2 and PDK4 are controlled in different ways. Several metabolic regulators, including forkhead box O1 (FoxO1), liver X receptor (LXR), peroxisome proliferator-activated receptor α (PPARα) and PPARγ coactivator α (PGC-1α), stimulate PDK2 and PDK4 expression levels (44,45). Furthermore, p53 tumor suppressor, a master regulator of genome stability and cell cycle, acts as a negative regulator of PDK2 expression (46).

In the present study, AG reduced PDK1-3 expression at both the mRNA and protein levels in a dose-dependent manner. AG inhibits the protein levels of HIF1α via the PI3K/Akt pathway and ubiquitin-mediated proteolysis (13,14). Thus, the

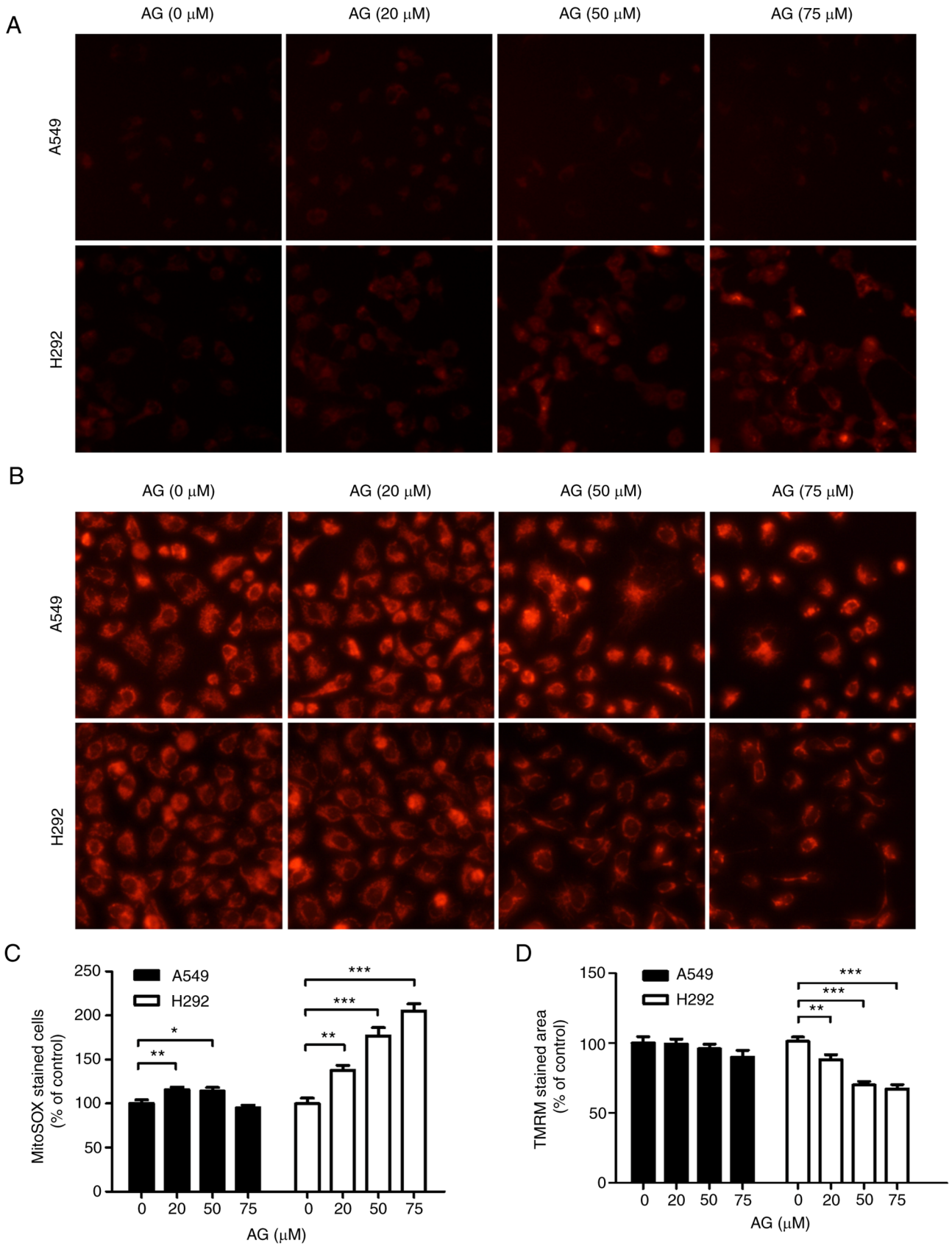

Figure 4. AG induces mitochondrial dysfunction. (A) A549 and H292 cells were treated with various concentrations of AG (20, 50 and 75 μM) for 6 h, and the mitochondrial ROS levels were measured using the MitoSox fluorescence dye. AG increased the levels of mitochondrial ROS in H292 cells, but not in A549 cells, in a dose-dependent manner. (B) Histogram showing the percentage of mitochondrial ROS levels in cells. Fluorescence intensity was calculated using the ImageJ software. AG significantly increased the ROS levels in H292 cells than that in A549 cells. (C) Histogram showing the mitochondrial membrane potential ratio of the AG treatment group to the control group using the tetramethylrhodamine methyl ester fluorescence dye. (D) AG induced mitochondrial damage in H292 cells via decrease in mitochondria membrane potential. A549 cells showed relatively very weak decrease in mitochondria membrane potential. Data are represented as the mean ± SD compared with the control from three independent experiments. *P<0.05, **P<0.01 and ***P<0.001 vs. control. AG, andrographolide; ROS, reactive oxygen species.

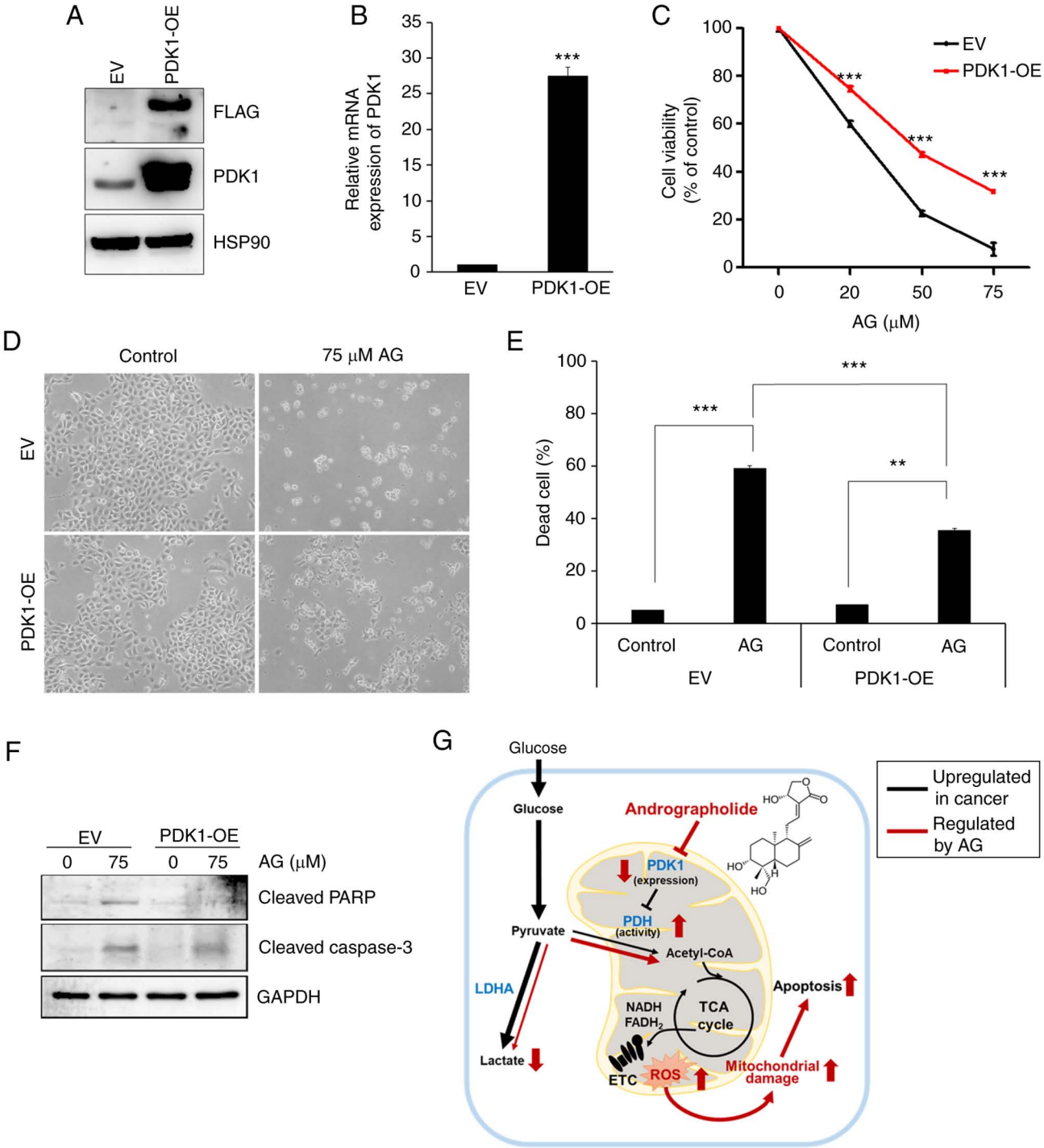

Figure 5. AG-induced cancer cell death is alleviated in PDK1-overexpressing H292 cells. (A) Overexpression of PDK1 protein in H292 cells was determined via western blotting. PDK1 expression vector was FLAG tagged to detect PDK1-overexpressing cells using an anti-FLAG antibody. (B) mRNA levels of PDK1 in H292 cells were determined via RT-qPCR. (C) After H292 cells were treated with AG, cell death was measured using the 3-(4,5-dimethylthiazol-2-yl)-2,5-diphenyl tetrazolium bromide (MTT) assay. AG-induced cell death was alleviated in PDK1-overexpressing H292 cells. (D) Morphological alterations revealed that PDK1-overexpressing H292 cells showed reduced apoptosis compared with the control cells. (E) Numbers of dead cells (combination of the Q1 + Q2) after AG treatment was measured via FACS analysis. A histogram showing the percentage of dead cells is produced by the analysis of 10,000 cells after AG treatment in PDK1-overexpressing and empty vector cells. (F) Activation of apoptotic signals by PARP and caspase-3 cleavage was examined via western blotting. The cleavage of PARP and caspase-3 was slightly weak in PDK1-overexpressing H292 cells. GAPDH was used as the internal control. (G) Mechanism of AG-induced cancer cell death via PDK1 inhibition. Data are represented as the mean ± SD compared with the control from three independent experiments. **P<0.01 and ***P<0.001 compared with each group. AG, andrographolide; PDK, pyruvate dehydrogenase kinase; PARP, cleaved poly (ADP ribose) polymerase; EV, empty vector; OE, overexpressing.

downregulation of PDK1 and PDK3 expression levels can be explained, at least in part, by an HIF1α-dependent pathway. However, the expression of another target of HIF1α for glycolysis, LDHA, was not altered by AG treatment. Extensive research is needed to determine the reason for the differential regulation of these genes. AG increases p53 expression levels

in several cancer lines (47-50) and decreases PPARγ expression levels in several metabolic diseases (51-53). Therefore, they may act as upstream regulators of PDK2 downregulation caused by AG treatment. Although the LXR, Myc and Wnt signaling pathways are associated with AG, their expression levels are increased by AG treatment (49,50,54). Therefore, it was concluded that these pathways cannot be the upstream regulators of PDK expression levels in AG-treated cancer cells. PubMed database search revealed that E2F1 and FoxO1 pathways were not previously identified as molecular targets for AG. The expression of PDK4 was not examined in the present study since it was not expressed in these cell lines and exerts a suppressive effect on tumorigenesis in several cancer types, including NSCLC (55,56).

Although AG treatment reduced the expression levels of all three isoforms (PDK1-3) in a dose-dependent manner, correlation analysis revealed that PDK1 may be the most potent target of AG among them. This possibility was evaluated by comparing the efficacy of AG in mitochondria-dependent apoptosis in A549 and H292 cells, which have vastly different PDK1 expression levels. PDK1-overexpressing cancers, particularly NSCLC (31,57), are resistant to chemotherapy and radiotherapy (58-60). In addition, PDK1 protects against apoptotic cell death by reducing OXPHOS, ROS production and mitochondrial membrane stability (57,60,61). As expected, H292 cells expressing high levels of PDK1 experienced more apoptotic cell death, mitochondrial ROS generation and MMP depletion than A549 cells expressing low levels of PDK1. PDK1-overexpressing H292 cells that exogenously expressed PDK1 regardless of AG treatment were generated to confirm the role of PDK1 in AG-induced apoptotic cell death. Exogenously overexpressed PDK1 is unaffected by AG regulation on PDK1 expression. Although PDK1 overexpression did not completely abolish the AG-induced apoptotic cell death, the portion of dead cell was significantly recovered by exogenous PDK1 overexpression, as demonstrated in a previous study by the authors (62). Based on these data, it was concluded that AG may have another target to induce apoptotic cell death in NSCLC, as reported in previous studies (9,10,63). Nonetheless, the present findings suggested that PDK1 overexpression partially reverses AG-induced cytotoxicity and apoptosis. To elucidate the precise mechanism of AG-stimulated apoptotic cell death, further studies should examine the upstream regulators that directly bind to AG and regulate multiple targets, along with the correlations between PDK1 and other proapoptotic factors.

In conclusion, it was revealed that AG induced mitochondria-mediated apoptosis in a PDK1-dependent manner. AG further inhibited PDK1 expression and increased PDH activity. Aerobic glycolysis was changed to mitochondrial OXPHOS in cancer cells. Moreover, PDK1-mediated metabolic shift resulted in mitochondrial ROS generation, MMP loss and apoptotic cell death. Therefore, PDK1-mediated metabolic change can explain AG-stimulated apoptotic cell death as a basis for its anticancer effect; however, this needs to be investigated further in future studies.

Acknowledgements

Not applicable.

Funding

The present study was supported by Basic Science Research Program through the National Research Foundation of Korea (NRF) funded by the Ministry of Education (grant no. NRF-2020R1I1A1A01068254) and by the National Research Foundation of Korea (NRF) grants funded by the Korea government (MIST) (grant nos. NRF-2022R1A2C2005130 and NRF-2021R1A4A1025662).

Availability of data and materials

The datasets used and/or analyzed during the current study are available from the corresponding author on reasonable request.

Authors' contributions

ESY and YD performed most of the experiments and data analysis and wrote the manuscript. TK and KTH conceived and designed the study and involved in writing the manuscript. SC performed the LDH assay. BK and JL constructed PDK1 overexpressing cells. MKC performed FACS analysis. SJB constructed PDK1 expressing vector. TK and SJB revised the manuscript. ESY, YD and KTH confirm the authenticity of all raw data. All authors read and approved the final manuscript.

Ethics approval and consent to participate

Not applicable.

Patient consent for publication

Not applicable.

Competing interests

The authors declare that they have no competing interests.

References

1. Hanahan D and Weinberg RA: Hallmarks of cancer: The next generation. Cell 144: 646-674, 2011.
2. Pavlova NN, Zhu J and Thompson CB: The hallmarks of cancer metabolism: Still emerging. Cell Metab 34: 355-377, 2022.
3. Altenberg B and Greulich KO: Genes of glycolysis are ubiquitously overexpressed in 24 cancer classes. Genomics 84: 1014-1020, 2004.
4. Jiang B: Aerobic glycolysis and high level of lactate in cancer metabolism and microenvironment. Genes Dis 4: 25-27, 2017.
5. DeBerardinis RJ, Lum JJ, Hatzivassiliou G and Thompson CB: The biology of cancer: Metabolic reprogramming fuels cell growth and proliferation. Cell Metab 7: 11-20, 2008.
6. Lin X, Xiao Z, Chen T, Liang SH and Guo H: Glucose metabolism on tumor plasticity, diagnosis, and treatment. Front Oncol 10: 317, 2020.
7. Woolbright BL, Rajendran G, Harris RA and Taylor JA III: Metabolic flexibility in cancer: Targeting the pyruvate dehydrogenase kinase: Pyruvate dehydrogenase axis. Mol Cancer Ther 18: 1673-1681, 2019.
8. Rajani M, Shrivastava N and Ravishankara MN: A rapid method for isolation of andrographolide from *Andrographis paniculata* nees (kalmegh). Pharm Biol 38: 204-209, 2000.
9. Farooqi AA, Attar R, Sabitaliyevich UY, Alaaeddine N, de Sousa DP, Xu B and Cho WC: The prowess of andrographolide as a natural weapon in the war against cancer. Cancers (Basel) 12: 2159, 2020.

10. Islam MT, Ali ES, Uddin SJ, Islam MA, Shaw S, Khan IN, Saravi SSS, Ahmad S, Rehman S, Gupta VK, *et al*: Andrographolide, a diterpene lactone from *Andrographis paniculata* and its therapeutic promises in cancer. Cancer Lett 420: 129-145, 2018.
11. Hocker HJ, Cho KJ, Chen CY, Rambahal N, Sagineedu SR, Shaari K, Stanslas J, Hancock JF and Gorfe AA: Andrographolide derivatives inhibit guanine nucleotide exchange and abrogate oncogenic Ras function. Proc Natl Acad Sci USA 110: 10201-10206, 2013.
12. Nguyen VS, Loh XY, Wijaya H, Wang J, Lin Q, Lam Y, Wong WS and Mok YK: Specificity and inhibitory mechanism of andrographolide and its analogues as antiasthma agents on NF-κB p50. J Nat Prod 78: 208-217, 2015.
13. Lin HH, Tsai CW, Chou FP, Wang CJ, Hsuan SW, Wang CK and Chen JH: Andrographolide down-regulates hypoxia-inducible factor-1α in human non-small cell lung cancer A549 cells. Toxicol Appl Pharmacol 250: 336-345, 2011.
14. Li J, Zhang C, Jiang H and Cheng J: Andrographolide inhibits hypoxia-inducible factor-1 through phosphatidylinositol 3-kinase/AKT pathway and suppresses breast cancer growth. Onco Targets Ther 8: 427-435, 2015.
15. Li GF, Qin YH and Du PQ: Andrographolide inhibits the migration, invasion and matrix metalloproteinase expression of rheumatoid arthritis fibroblast-like synoviocytes via inhibition of HIF-1α signaling. Life Sci 136: 67-72, 2015.
16. Lin HC, Su SL, Lu CY, Lin AH, Lin WC, Liu CS, Yang YC, Wang HM, Lii CK and Chen HW: Andrographolide inhibits hypoxia-induced HIF-1α-driven endothelin 1 secretion by activating Nrf2/HO-1 and promoting the expression of prolyl hydroxylases 2/3 in human endothelial cells. Environ Toxicol 32: 918-930, 2017.
17. Chen Z, Tang WJ, Zhou YH, Chen ZM and Liu K: Andrographolide inhibits non-small cell lung cancer cell proliferation through the activation of the mitochondrial apoptosis pathway and by reprogramming host glucose metabolism. Ann Transl Med 9: 1701, 2021.
18. Li X, Tian R, Liu L, Wang L, He D, Cao K, Ma JK and Huang C: Andrographolide enhanced radiosensitivity by downregulating glycolysis via the inhibition of the PI3K-Akt-mTOR signaling pathway in HCT116 colorectal cancer cells. J Int Med Res 48: 300060520946169, 2020.
19. Devkota AK, Kaoud TS, Warthaka M and Dalby KN: Fluorescent peptide assays for protein kinases. Curr Protoc Mol Biol Chapter 18: Unit 18.17, 2010.
20. Mullinax TR, Stepp LR, Brown JR and Reed LJ: Synthetic peptide substrates for mammalian pyruvate dehydrogenase kinase and pyruvate dehydrogenase phosphatase. Arch Biochem Biophys 243: 655-659, 1985.
21. Livak KJ and Schmittgen TD: Analysis of relative gene expression data using real-time quantitative PCR and the 2(-Delta Delta C(T)) method. Methods 25: 402-408, 2001.
22. Anwar S, Shamsi A, Mohammad T, Islam A and Hassan MI: Targeting pyruvate dehydrogenase kinase signaling in the development of effective cancer therapy. Biochim Biophys Acta Rev Cancer 1876: 188568, 2021.
23. Yadav N, Kumar S, Marlowe T, Chaudhary AK, Kumar R, Wang J, O'Malley J, Boland PM, Jayanthi S, Kumar TK, *et al*: Oxidative phosphorylation-dependent regulation of cancer cell apoptosis in response to anticancer agents. Cell Death Dis 6: e1969, 2015.
24. Michelakis ED, Webster L and Mackey JR: Dichloroacetate (DCA) as a potential metabolic-targeting therapy for cancer. Br J Cancer 99: 989-994, 2008.
25. McFate T, Mohyeldin A, Lu H, Thakar J, Henriques J, Halim ND, Wu H, Schell MJ, Tsang TM, Teahan O, *et al*: Pyruvate dehydrogenase complex activity controls metabolic and malignant phenotype in cancer cells. J Biol Chem 283: 22700-22708, 2008.
26. Wang X, Shen X, Yan Y and Li H: Pyruvate dehydrogenase kinases (PDKs): An overview toward clinical applications. Biosci Rep 41: BSR20204402, 2021.
27. Hur H, Xuan Y, Kim YB, Lee G, Shim W, Yun J, Ham IH and Han SU: Expression of pyruvate dehydrogenase kinase-1 in gastric cancer as a potential therapeutic target. Int J Oncol 42: 44-54, 2013.
28. Fujiwara S, Kawano Y, Yuki H, Okuno Y, Nosaka K, Mitsuya H and Hata H: PDK1 inhibition is a novel therapeutic target in multiple myeloma. Br J Cancer 108: 170-178, 2013.
29. Tan J, Lee PL, Li Z, Jiang X, Lim YC, Hooi SC and Yu Q: B55β-associated PP2A complex controls PDK1-directed myc signaling and modulates rapamycin sensitivity in colorectal cancer. Cancer Cell 18: 459-471, 2010.
30. Qu C, Yan C, Cao W, Li F, Qu Y, Guan K, Si C, Yu Z and Qu Z: miR-128-3p contributes to mitochondrial dysfunction and induces apoptosis in glioma cells via targeting pyruvate dehydrogenase kinase 1. IUBMB Life 72: 465-475, 2020.
31. Liu T and Yin H: PDK1 promotes tumor cell proliferation and migration by enhancing the Warburg effect in non-small cell lung cancer. Oncol Rep 37: 193-200, 2017.
32. Zhang W, Hu X, Chakravarty H, Yang Z and Tam KY: Identification of novel pyruvate dehydrogenase kinase 1 (PDK1) inhibitors by kinase activity-based high-throughput screening for anticancer therapeutics. ACS Comb Sci 20: 660-671, 2018.
33. Garon EB, Christofk HR, Hosmer W, Britten CD, Bahng A, Crabtree MJ, Hong CS, Kamranpour N, Pitts S, Kabbinavar F, *et al*: Dichloroacetate should be considered with platinum-based chemotherapy in hypoxic tumors rather than as a single agent in advanced non-small cell lung cancer. J Cancer Res Clin Oncol 140: 443-452, 2014.
34. Yang Z, Zhang SL, Hu X and Tam KY: Inhibition of pyruvate dehydrogenase kinase 1 enhances the anti-cancer effect of EGFR tyrosine kinase inhibitors in non-small cell lung cancer. Eur J Pharmacol 838: 41-52, 2018.
35. Jin L, Kim EY, Chung TW, Han CW, Park SY, Han JH, Bae SJ, Lee JR, Kim YW, Jang SB and Ha KT: Hemistepsin A suppresses colorectal cancer growth through inhibiting pyruvate dehydrogenase kinase activity. Sci Rep 10: 21940, 2020.
36. Kwak CH, Jin L, Han JH, Han CW, Kim E, Cho M, Chung TW, Bae SJ, Jang SB and Ha KT: Ilimaquinone induces the apoptotic cell death of cancer cells by reducing pyruvate dehydrogenase kinase 1 activity. Int J Mol Sci 21: 6021, 2020.
37. Kwak CH, Lee JH, Kim EY, Han CW, Kim KJ, Lee H, Cho M, Jang SB, Kim CH, Chung TW and Ha KT: Huzhangoside A suppresses tumor growth through inhibition of pyruvate dehydrogenase kinase activity. Cancers (Basel) 11: 712, 2019.
38. Alapid AAI, Abd Majid R, Ibraheem ZO, Mediani A, Ismail IS, Unyah NZ, Alhassan Abdullahi S, Nordin N, Nasiru Wana M and Basir R: Investigation of andrographolide effect on non-infected red blood cells using the 1H-NMR-based metabolomics approach. Metabolites 11: 486, 2021.
39. Kim JW, Tchernyshyov I, Semenza GL and Dang CV: HIF-1-mediated expression of pyruvate dehydrogenase kinase: A metabolic switch required for cellular adaptation to hypoxia. Cell Metab 3: 177-185, 2006.
40. Papandreou I, Cairns RA, Fontana L, Lim AL and Denko NC: HIF-1 mediates adaptation to hypoxia by actively downregulating mitochondrial oxygen consumption. Cell Metab 3: 187-197, 2006.
41. Wang LY, Hung CL, Chen YR, Yang JC, Wang J, Campbell M, Izumiya Y, Chen HW, Wang WC, Ann DK and Kung HJ: KDM4A coactivates E2F1 to regulate the PDK-dependent metabolic switch between mitochondrial oxidation and glycolysis. Cell Rep 16: 3016-3027, 2016.
42. Kim JW, Gao P, Liu YC, Semenza GL and Dang CV: Hypoxia-inducible factor 1 and dysregulated c-Myc cooperatively induce vascular endothelial growth factor and metabolic switches hexokinase 2 and pyruvate dehydrogenase kinase 1. Mol Cell Biol 27: 7381-7393, 2007.
43. Pate KT, Stringari C, Sprowl-Tanio S, Wang K, TeSlaa T, Hoverter NP, McQuade MM, Garner C, Digman MA, Teitell MA, *et al*: Wnt signaling directs a metabolic program of glycolysis and angiogenesis in colon cancer. EMBO J 33: 1454-1473, 2014.
44. Piao L, Sidhu VK, Fang YH, Ryan JJ, Parikh KS, Hong Z, Toth PT, Morrow E, Kutty S, Lopaschuk GD and Archer SL: FOXO1-mediated upregulation of pyruvate dehydrogenase kinase-4 (PDK4) decreases glucose oxidation and impairs right ventricular function in pulmonary hypertension: Therapeutic benefits of dichloroacetate. J Mol Med (Berl) 91: 333-346, 2013.
45. Sugden MC and Holness MJ: Mechanisms underlying regulation of the expression and activities of the mammalian pyruvate dehydrogenase kinases. Arch Physiol Biochem 112: 139-149, 2006.
46. Contractor T and Harris CR: p53 negatively regulates transcription of the pyruvate dehydrogenase kinase Pdk2. Cancer Res 72: 560-567, 2012.
47. Gao H, Li H, Liu W, Mishra SK and Li C: Andrographolide induces apoptosis in gastric cancer cells through reactivation of p53 and inhibition of Mdm-2. Dokl Biochem Biophys 500: 393-401, 2021.
48. Shi MD, Lin HH, Lee YC, Chao JK, Lin RA and Chen JH: Inhibition of cell-cycle progression in human colorectal carcinoma Lovo cells by andrographolide. Chem Biol Interact 174: 201-210, 2008.

49. Othman NS and Mohd Azman DK: Andrographolide induces G2/M cell cycle arrest and apoptosis in human glioblastoma DBTRG-05MG cell line via ERK1/2/c-Myc/p53 signaling pathway. Molecules 27: 6686, 2022.
50. Zhang J, Li C, Zhang L, Heng Y, Wang S, Pan Y, Cai L, Zhang Y, Xu T, Chen X, *et al*: Andrographolide, a diterpene lactone from the traditional Chinese medicine andrographis paniculate, induces senescence in human lung adenocarcinoma via p53/p21 and Skp2/p27. Phytomedicine 98: 153933, 2022.
51. Jin L, Fang W, Li B, Shi G, Li X, Yang Y, Yang J, Zhang Z and Ning G: Inhibitory effect of andrographolide in 3T3-L1 adipocytes differentiation through the PPARγ pathway. Mol Cell Endocrinol 358: 81-87, 2012.
52. Lin HC, Lii CK, Chen HC, Lin AH, Yang YC and Chen HW: Andrographolide inhibits oxidized LDL-induced cholesterol accumulation and foam cell formation in macrophages. Am J Chin Med 46: 87-106, 2018.
53. Shu J, Huang R, Tian Y, Liu Y, Zhu R and Shi G: Andrographolide protects against endothelial dysfunction and inflammatory response in rats with coronary heart disease by regulating PPAR and NF-κB signaling pathways. Ann Palliat Med 9: 1965-1975, 2020.
54. Tapia-Rojas C, Schuller A, Lindsay CB, Ureta RC, Mejías-Reyes C, Hancke J, Melo F and Inestrosa NC: Andrographolide activates the canonical Wnt signalling pathway by a mechanism that implicates the non-ATP competitive inhibition of GSK-3β: Autoregulation of GSK-3β in vivo. Biochem J 466: 415-430, 2015.
55. Li G, Li M, Hu J, Lei R, Xiong H, Ji H, Yin H, Wei Q and Hu G: The microRNA-182-PDK4 axis regulates lung tumorigenesis by modulating pyruvate dehydrogenase and lipogenesis. Oncogene 36: 989-998, 2017.
56. Atas E, Oberhuber M and Kenner L: The implications of PDK1-4 on tumor energy metabolism, aggressiveness and therapy resistance. Front Oncol 10: 583217, 2020.
57. De Rosa V, Iommelli F, Terlizzi C, Leggiero E, Camerlingo R, Altobelli GG, Fonti R, Pastore L and Del Vecchio S: Non-canonical role of PDK1 as a negative regulator of apoptosis through macromolecular complexes assembly at the ER-mitochondria interface in oncogene-driven NSCLC. Cancers (Basel) 13: 4133, 2021.
58. Yao S, Shang W, Huang L, Xu R, Wu M and Wang F: The oncogenic and prognostic role of PDK1 in the progression and metastasis of ovarian cancer. J Cancer 12: 630-643, 2021.
59. Peng F, Wang JH, Fan WJ, Meng YT, Li MM, Li TT, Cui B, Wang HF, Zhao Y, An F, *et al*: Glycolysis gatekeeper PDK1 reprograms breast cancer stem cells under hypoxia. Oncogene 37: 1119, 2018.
60. Lu H, Lu Y, Xie Y, Qiu S, Li X and Fan Z: Rational combination with PDK1 inhibition overcomes cetuximab resistance in head and neck squamous cell carcinoma. JCI Insight 4: e131106, 2019.
61. Jin L, Cho M, Kim BS, Han JH, Park S, Lee IK, Ryu D, Kim JH, Bae SJ and Ha KT: Drug evaluation based on phosphomimetic PDHA1 reveals the complexity of activity-related cell death in A549 non-small cell lung cancer cells. BMB Rep 54: 563-568, 2021.
62. Kim BS, Chung TW, Choi HJ, Bae SJ, Cho HR, Lee SO, Choi JH, Joo JK and Ha KT: Caesalpinia sappan induces apoptotic cell death in ectopic endometrial 12Z cells through suppressing pyruvate dehydrogenase kinase 1 expression. Exp Ther Med 21: 357, 2021.
63. Zeng B, Wei A, Zhou Q, Yuan M, Lei K, Liu Y, Song J, Guo L and Ye Q: Andrographolide: A review of its pharmacology, pharmacokinetics, toxicity and clinical trials and pharmaceutical researches. Phytother Res 36: 336-364, 2022.